β-$FeSi_2$ as the bottom absorber of triple-junction thin-film solar cells: A numerical study*

Yuan Ji-Ren(袁吉仁)[a)b)c)†], Shen Hong-Lie(沈鸿烈)[b)], Zhou Lang(周 浪)[a)], Huang Hai-Bin(黄海宾)[a)], Zhou Nai-Gen(周耐根)[a)], Deng Xin-Hua(邓新华)[c)], and Yu Qi-Ming(余启名)[c)]

[a)] *School of Materials Science and Engineering, Nanchang University, Nanchang* 330031, *China*
[b)] *College of Materials Science and Technology, Nanjing University of Aeronautics and Astronautics, Nanjing* 210016, *China*
[c)] *School of Science, Nanchang University, Nanchang* 330031, *China*

(Received 22 October 2013; revised manuscript received 27 November 2013; published online 24 January 2014)

Using β-$FeSi_2$ as the bottom absorber of triple-junction thin-film solar cells is investigated by a numerical method for widening the long-wave spectral response. The presented results show that the β-$FeSi_2$ subcell can contribute 0.273 V of open-circuit voltage to the a-Si/μc-Si/β-$FeSi_2$ triple-junction thin-film solar cell. The optimized absorber thicknesses for a-Si, μc-Si, and β-$FeSi_2$ subcells are 260 nm, 900 nm, and 40 nm, respectively. In addition, the temperature coefficient of the conversion efficiency of the a-Si/μc-Si/β-$FeSi_2$ cell is -0.308 %/K, whose absolute value is only greater than that of the a-Si subcell. This result indicates that the a-Si/μc-Si/β-$FeSi_2$ triple-junction solar cell has a good temperature coefficient. As a result, using β-$FeSi_2$ as the bottom absorber can improve the thin-film solar cell performance, and the a-Si/μc-Si/β-$FeSi_2$ triple-junction solar cell is a promising structure configuration for improving the solar cell efficiency.

Keywords: β-$FeSi_2$, solar cell, temperature coefficient, conversion efficiency

PACS: 88.40.hj, 88.40.jp, 88.30.gg **DOI:** 10.1088/1674-1056/23/3/038801

1. Introduction

Semiconducting iron disilicide (β-$FeSi_2$) has attracted considerable attention due to its remarkable optical and electrical properties.[1–4] β-$FeSi_2$ has a very high optical absorption coefficient ($\alpha > 10^5$ cm^{-1}), which is at least two orders of magnitude larger than that of crystalline silicon at 1.5 eV.[5,6] It is also compatible with the silicon-process technology. Moreover, β-$FeSi_2$ is an ecofriendly material because its element resources (Fe and Si) are non-toxic and abundant in the earth's crust. Thus, β-$FeSi_2$ is one of the most promising absorber materials for thin-film solar cells.

Recently, photovoltaics employing β-$FeSi_2$ have already been reported.[7–12] However, there are limited studies on the single-junction solar cells. In this paper, we propose an a-Si/μc-Si/β-$FeSi_2$ triple-junction thin-film solar cell in which β-$FeSi_2$ is used as the absorber material of the bottom cell, the long-wave spectral response will be widened from 1100 nm in the a-Si/μc-Si tandem structure to above 1400 nm in this triple-junction solar cell. Higher efficiencies are expected for triple-junction thin-film solar cells. The a-Si/μc-Si/β-$FeSi_2$ triple-junction solar cell is particularly attractive since there is no need for lattice matching. The tunnel junctions of this triple-junction solar cell can also be efficiently made by a-Si and μc-Si materials.[13,14] Moreover, this triple-junction solar cell possesses a good thermal property due to the compatibility of the preparation process and their similar thermal expansion coefficients.[15,16] In this paper, a theoretical study of the a-Si/μc-Si/β-$FeSi_2$ triple-junction thin-film solar cell is carried out by using the device simulator AMPS-1D.[17] The influences of the subcell thickness and the operating temperature on the cell performance are investigated. The potential conversion efficiency of the triple-junction thin-film solar cell is discussed.

2. Methodologies

We introduce computer program AMPS-1D,[17] which is based on the Poisson equation and the hole and electron continuity equations, to perform the numerical analysis of the a-Si/μc-Si/β-$FeSi_2$ triple-junction thin-film solar cell. The a-Si/μc-Si/β-$FeSi_2$ triple-junction solar cell is constituted by p–i–n type a-Si, μc-Si, and β-$FeSi_2$ subcells and its structural configuration is shown in Fig. 1. The density of localized states in the mobility bandgap of a-Si is assumed to be both acceptor-like states and donor-like states modeled by exponential band tails (Urbach tails) and Gaussian mid-gap states (associated with silicon dangling bonds). For μc-Si, the density of localized states in the mobility bandgap is assumed to be both acceptor-like states and donor-like states modeled

*Project supported by the National Natural Science Foundation of China (Grant Nos. 61176062, 61306084, and 51361022), the Priority Academic Program Development of Jiangsu Higher Education Institutions, China, the Ph. D. Program Foundation of Ministry of Education of China (Grant No. 20113601120006), the Natural Science Foundation of Jiangxi Province, China (Grant No. 20122BAB202002), and the Science and Technology Project of Education Department of Jiangxi Province, China (Grant No. GJJ13010).

†Corresponding author. E-mail: yuanjiren@ncu.edu.cn

© 2014 Chinese Physical Society and IOP Publishing Ltd

by exponential band tails and flat mid-gap states. The material parameters of a-Si, μc-Si, and β-$FeSi_2$ are taken from Refs. [18]–[20], [20] and [21], and [9] and [10], respectively, and some basic material parameters are listed in Tables 1–3. The light absorption coefficients of a-Si and μc-Si are taken from Refs. [22] and [23], respectively. The light absorption coefficient of β-$FeSi_2$ has been given in our previous work.[9] The temperature coefficients of the bandgaps of a-Si, μc-Si, and β-$FeSi_2$ are 4.7×10^{-4} eV/K,[24] 4.2×10^{-4} eV/K,[25] and 3.1×10^{-4} eV/K,[26] respectively. The Yunaz model[27,28] of the tunnel-recombination junction for simulating the triple-junction solar cell is employed. The simulated illumination is AM 1.5G, 100 mW/cm^2. The reflection indices for the forward and the reverse directions are set to 0.1 and 0.6, respectively.

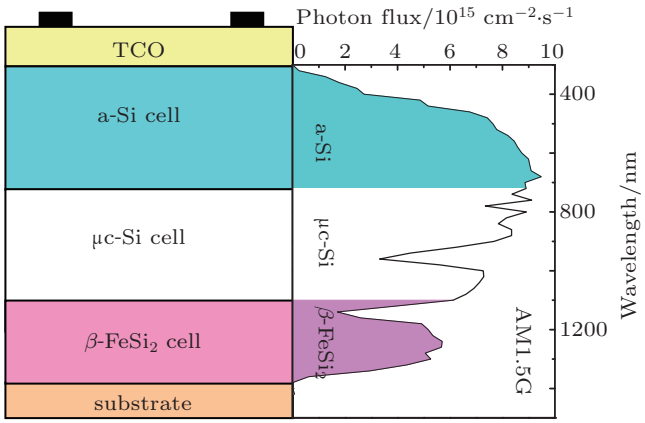


Fig. 1. (color online) Schematic structure of a-Si/μc-Si/β-$FeSi_2$ triple-junction thin-film solar cell and the cut-off wavelengths of the spectral responses of a-Si, μc-Si, and β-$FeSi_2$ subcells.

Table 1. Basic parameters of a-Si at 300 K used in this study.

Parameter	a-SiC (p)	a-Si (i)	a-Si (n)
Layer thickness/nm	10	varied	10
Relative dielectric constant	11.9	11.9	11.9
Electron affinity/eV	3.7	3.8	3.8
Mobility bandgap/eV	1.96	1.82	1.82
Optical bandgap/eV	1.80	1.72	1.72
Effective conduction band density/cm^{-3}	2.5×10^{20}	2.5×10^{20}	2.5×10^{20}
Effective valence band density/cm^{-3}	2.5×10^{20}	2.5×10^{20}	2.5×10^{20}
Donor/acceptor concentration/cm^{-3}	3×10^{19}	–	3×10^{19}
Electron mobility/cm$^2\cdot$V$^{-1}\cdot$s^{-1}	10	20	20
Hole mobility/cm$^2\cdot$V$^{-1}\cdot$s^{-1}	1	2	2

Table 2. Basic parameters of μc-Si at 300 K used in this study.

Parameters and units	μc-Si (p)	μc-Si (i)	μc-Si (n)
Layer thickness/nm	10	varied	10
Relative dielectric constant	11.9	11.9	11.9
Electron affinity/eV	4.0	4.0	4.0
Mobility bandgap/eV	1.30	1.30	1.30
Optical bandgap/eV	1.12	1.12	1.12
Effective conduction band density/cm^{-3}	3×10^{19}	3×10^{19}	3×10^{19}
Effective valence band density/cm^{-3}	2×10^{19}	2×10^{19}	2×10^{19}
Donor/acceptor concentration/cm^{-3}	1×10^{19}	–	1×10^{19}
Electron mobility/cm$^2\cdot$V$^{-1}\cdot$s^{-1}	40	40	40
Hole mobility/cm$^2\cdot$V$^{-1}\cdot$s^{-1}	4	4	4

Table 3. Basic parameters of β-$FeSi_2$ at 300 K used in this study.

Parameters and units	β-$FeSi_2$ (p)	β-$FeSi_2$ (i)	β-$FeSi_2$ (n)
Layer thickness/nm	10	varied	10
Relative dielectric constant	31	31	31
Electron affinity/eV	3.86	3.86	3.86
Mobility bandgap/eV	0.87	0.87	0.87
Optical bandgap/eV	0.87	0.87	0.87
Effective conduction band density/cm^{-3}	2.5×10^{19}	2.5×10^{19}	2.5×10^{19}
Effective valence band density/cm^{-3}	2.5×10^{19}	2.5×10^{19}	2.5×10^{19}
Donor/acceptor concentration/cm^{-3}	5×10^{18}	1×10^{16}	3×10^{18}
Electron mobility/cm$^2\cdot$V$^{-1}\cdot$s^{-1}	70	70	70
Hole mobility/cm$^2\cdot$V$^{-1}\cdot$s^{-1}	20	20	20

3. Results and discussion

3.1. Effect of subcell absorber thickness

A design principle of multi-junction cells is that the absorption spectral distribution of each subcell is reasonable to make each subcell having the same photocurrent. The photocurrent of each subcell is related to the absorber (i layer) thickness. The absorber thickness for each subcell should be optimized. We calculate the short-circuit current density (J_{sc}) for each subcell after the absorber thicknesses for the subcells are set to certain values. If the short-circuit current density for a subcell is at minimum, its absorber thickness will be adjusted. In this way, the optimal absorber thicknesses for a-Si, μc-Si and β-$FeSi_2$ are found to be 260 nm, 900 nm, and 40 nm, respectively. Figure 2 shows the short-circuit current density of each subcell when three subcells have the same photocurrent (current matching condition). Figure 3 shows the current-voltage characteristics of a-Si/μc-Si/β-$FeSi_2$ solar cell after optimizing the cell absorber thicknesses. The conversion efficiency η, the short-circuit current density, the open-circuit voltage V_{oc}, and the fill factor (FF) are 19.80%, 13.31 mA/cm^2, 1.962 V, and 0.762, respectively. It should be mentioned that the optimized a-Si/μc-Si tandem solar cell has a lab efficiency of 11.04%.[29] The world record for the highest efficiency of the a-Si/μc-Si tandem solar cell is 12.3%.[30] So, the β-$FeSi_2$ subcell can give much contribution to the cell efficiency.

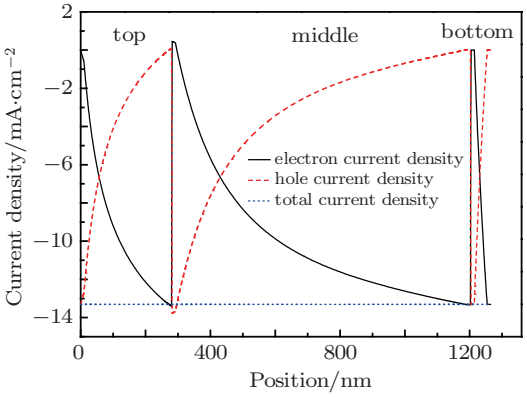


Fig. 2. (color online) Short-circuit current density of each subcell under current matching condition.

Figure 4 illustrates the influence of the a-Si absorber thickness on the cell performance when the absorber thicknesses of μc-Si and β-$FeSi_2$ are 900 nm and 40 nm, respectively. It is found that the short-circuit current density increases when the a-Si absorber thickness increases from 220 nm to 260 nm. As the a-Si absorber thickness increases, more photocarriers can be produced to contribute to the current. When the a-Si absorber is thicker than 260 nm, J_{sc} decreases with increasing a-Si absorber thickness since the collection efficiency of the photocarriers decreases due to the thicker absorber. The V_{oc} decreases slowly when the a-Si absorber thickness increases from 220 nm to 480 nm. The decrease of V_{oc} should come from the increase of recombination. The FF reaches the lowest value when the a-Si absorber thickness is 260 nm. The FF of the triple cell depends sensitively on the FF of the limiting subcell and the limiting subcell has a low FF.[14] A large mismatch of subcell currents can lead to a higher triple-cell FF. So, the FF has a minimum value at the optimized thickness. According to the above tendencies of J_{sc}, V_{oc}, and FF, the cell conversion efficiency increases first and then decreases with increasing a-Si absorber thickness. The η is maximum when the a-Si absorber thickness is 260 nm.

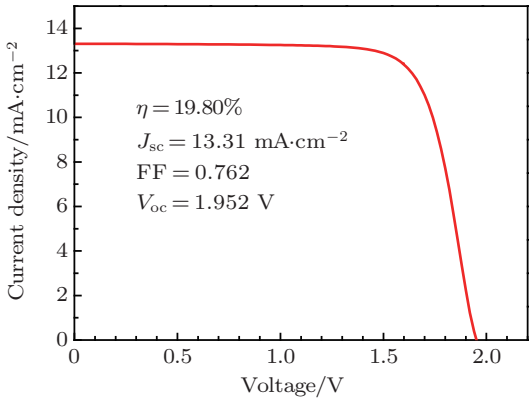


Fig. 3. (color online) Current-voltage characteristics of a-Si/μc-Si/β-$FeSi_2$ solar cell after optimizing the cell absorber thicknesses.

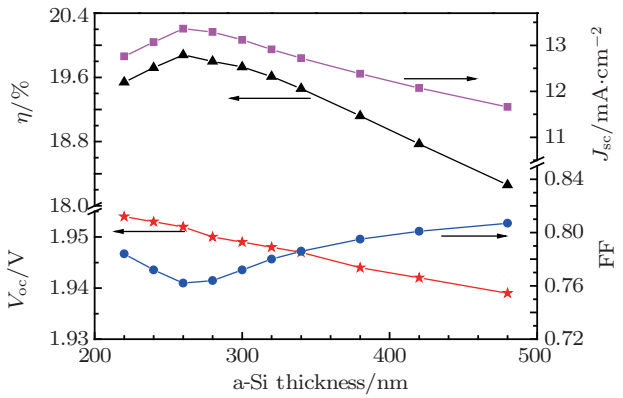


Fig. 4. (color online) Influence of a-Si absorber thickness on the cell performance when the absorber thicknesses of μc-Si and β-$FeSi_2$ are 900 nm and 40 nm, respectively.

Figure 5 shows the effect of the μc-Si absorber thickness on the cell property when the absorber thicknesses of a-Si and β-$FeSi_2$ are 260 nm and 40 nm, respectively. It is found that η and J_{sc} increase when the μc-Si absorber thickness increases from 500 nm to 900 nm, and they decrease when the μc-Si absorber thickness increases from 900 nm to 2000 nm. The V_{oc} decreases slowly with increasing μc-Si absorber thickness. The FF has the lowest value when the μc-Si absorber thickness is 900 nm. The cause of the changing tendency of J_{sc}, V_{oc}, and FF of μc-Si should be same as that of a-Si.

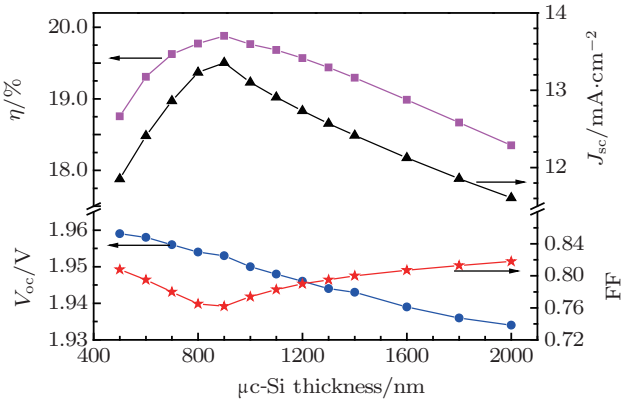


Fig. 5. (color online) Effect of μc-Si absorber thickness on the cell property when the absorber thicknesses of a-Si and β-$FeSi_2$ are 260 nm and 40 nm, respectively.

Figure 6 depicts the cell performance of a-Si/μc-Si/β-$FeSi_2$ with varying β-$FeSi_2$ absorber thickness when the absorber thicknesses of a-Si and μc-Si are 260 nm and 900 nm, respectively. It is observed that η and J_{sc} have saturation values when the β-$FeSi_2$ absorber thickness increases to 40 nm. The V_{oc} increases slightly with increasing β-$FeSi_2$ absorber thickness from 20 nm to 100 nm. A minimum is obtained for the FF when the β-$FeSi_2$ absorber thickness is 40 nm.

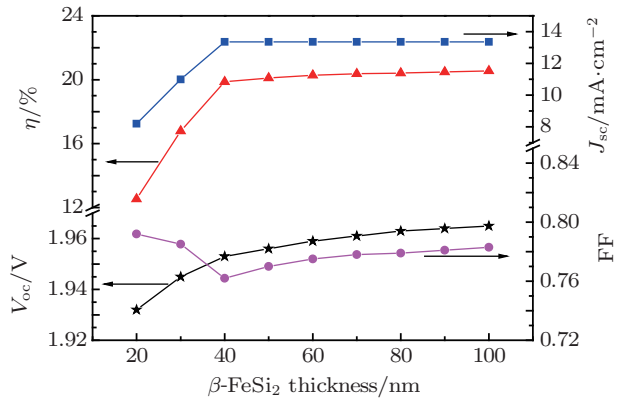


Fig. 6. (color online) Cell performance of a-Si/μc-Si/β-$FeSi_2$ with varying β-$FeSi_2$ absorber thickness when the absorber thicknesses of a-Si and μc-Si are 260 nm and 900 nm, respectively.

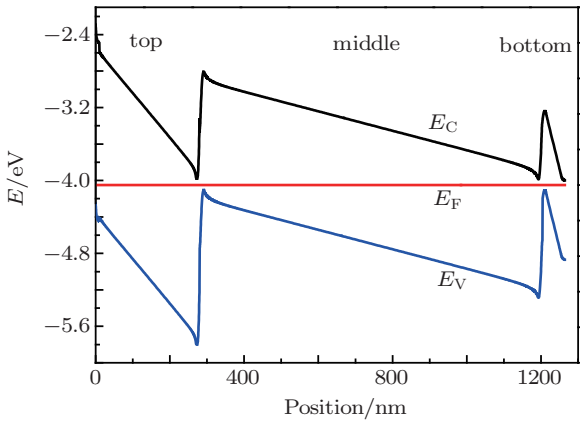


Fig. 7. (color online) Energy band diagram of a-Si/μc-Si/β-$FeSi_2$ solar cell at the thermal equilibrium state when all absorber thicknesses are optimized.

Figures 7 and 8 describe the energy band diagrams of the a-Si/μc-Si/β-$FeSi_2$ solar cell at the thermal equilibrium state and under the open-circuit condition when all absorber thicknesses are optimized. It is found that the β-$FeSi_2$ subcell can contribute 0.273 V of open-circuit voltage to the total V_{oc}. This result demonstrates that using β-$FeSi_2$ as the bottom absorber can improve the thin-film solar cell performance.

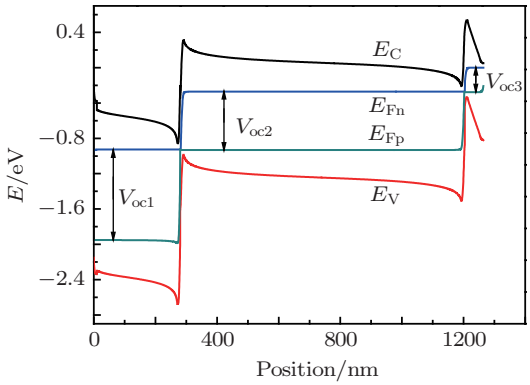


Fig. 8. (color online) Energy band diagram of a-Si/μc-Si/β-$FeSi_2$ solar cell under the open-circuit condition when all absorber thicknesses are optimized.

3.2. Effect of operating temperature

The performance of solar cells is usually tested under the conditions of 25 °C, AM1.5, and 100 mW/cm^2. However, in practice, the cell operating temperature varies in a broad range depending on the region or location where they are installed. When solar cells are operated outdoors, the module temperature increases, and sometimes it can reach over 70 °C in the daylight of a sunny day.[31] In this section, the effect of the operating temperature on the a-Si/μc-Si/β-$FeSi_2$ cell performance is discussed.

To analyze the temperature dependence of the solar cells, the operating temperature of the solar cells is varied from 298 K to 368 K. In our calculations, the temperature dependences of the bandgap and the absorption coefficient of each layer are also considered. The absorption coefficient of each layer is calculated using the Tauc model.[32] The bandgaps of a-Si, μc-Si, and β-$FeSi_2$ are calculated according to the equation

$$E_g(T) = E_g(300\ \mathrm{K}) + \frac{\mathrm{d}E_g}{\mathrm{d}T}(T - 300\ \mathrm{K}), \quad (1)$$

where $\mathrm{d}E_g/\mathrm{d}T$ is the bandgap temperature coefficient. The absorber thicknesses of a-Si, μc-Si, and β-$FeSi_2$ are 260 nm, 900 nm, and 40 nm, respectively.

The temperature coefficient of the conversion efficiency can be defined as

$$C_T = \frac{1}{\eta\,(T = 298\ \mathrm{K})}\frac{\mathrm{d}\eta}{\mathrm{d}T} \times 100\%, \quad (2)$$

where C_T is the temperature coefficient in units of %/K. The normalizing temperature is chosen to be 298 K because it corresponds to the standard reference condition for the solar cell performance.

Figure 9 shows the temperature coefficients of the conversion efficiencies of the a-Si/μc-Si/β-$FeSi_2$ cell and all subcells. It can be seen that the temperature coefficient of the conversion efficiency of the a-Si subcell is −0.254 %/K, whose absolute value is the smallest; that of the μc-Si subcell is −0.350 %/K; and that of β-$FeSi_2$ is −0.766 %/K, whose absolute value is the largest. The temperature coefficient of the conversion efficiency of the a-Si/μc-Si/β-$FeSi_2$ cell is −0.308 %/K, whose absolute value is only greater than that of the a-Si subcell. This result indicates that the a-Si/μc-Si/β-$FeSi_2$ triple-junction solar cell has a good temperature coefficient and it is a good structure for use in high-temperature or tropical regions.

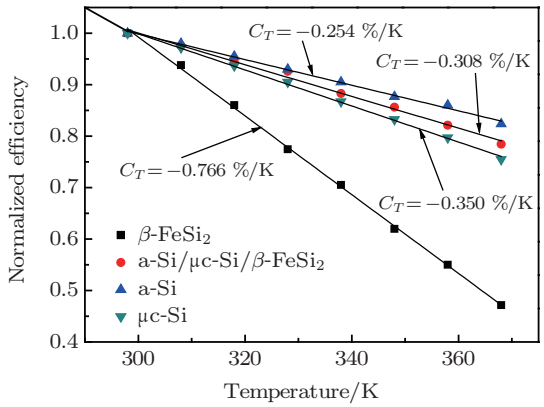


Fig. 9. (color online) Temperature coefficients of the conversion efficiencies of the a-Si/μc-Si/β-$FeSi_2$ cell and all subcells.

3.3. Evaluation of potential efficiency

The cut-off wavelengths of the spectral responses of a-Si, μc-Si, and β-$FeSi_2$ subcells are 720 nm, 1100 nm, and 1420 nm, respectively, as shown in Fig. 1. The whole range of the spectral response is very wide, spanning from the ultraviolet region to the near infrared waveband. It is expected that the a-Si/μc-Si/β-$FeSi_2$ triple-junction solar cell can reach a very high conversion efficiency. According to Ref. [33], the maximum theoretical efficiency for this triple-junction solar cell can achieve about 50% under AM1.5 direct normal irradiance, 1 sun. In Subsection 3.1, the conversion efficiency for the optimized cell is only 19.80%, far below the theoretical value. The low efficiency is attributed to the high density of localized states of a-Si and μc-Si. The density of localized states set in this calculation is taken from Ref. [20], in which the data are in agreement with the present experimental values. Obviously, these values would be improved with a better technological process. If we can minimize the density of localized states of a-Si and μc-Si by an advanced fabrication technology, the conversion efficiency of this triple-junction solar cell would reach a very high value. Also, the preparation of the β-$FeSi_2$ films on non-silicon substrates should be improved for fabricating a low-cost and high-efficiency a-Si/μc-Si/β-$FeSi_2$ triple-junction thin-film solar cell.

4. Conclusion

β-$FeSi_2$ has been employed as the bottom absorber of triple-junction thin-film solar cells. It is found that a conversion efficiency of 19.80% for the a-Si/μc-Si/β-$FeSi_2$ solar cell can be obtained and an increase of 0.273 V in open-circuit voltage can be realized by adding the β-$FeSi_2$ subcell. The optimized absorber thicknesses for a-Si, μc-Si, and β-$FeSi_2$ subcells are 260 nm, 900 nm, and 40 nm, respectively. The a-Si/μc-Si/β-$FeSi_2$ cell has a good temperature coefficient of the conversion efficiency (-0.308 %/K). A very high conversion efficiency of the a-Si/μc-Si/β-$FeSi_2$ thin-film cell may be achieved if we can further improve the preparation technology of a-Si, μc-Si, and β-$FeSi_2$ films. The results indicate that the a-Si/μc-Si/β-$FeSi_2$ structure is a promising configuration for high-efficient solar cells.

References

[1] Bost M C and Mahan J E 1988 *J. Appl. Phys.* **64** 2034
[2] Christensen N E 1990 *Phys. Rev. B* **42** 7148
[3] Powalla M and Herz K 1993 *Appl. Surf. Sci.* **65/66** 482
[4] Leong D, Harry M, Reeson K J and Homewood K P 1997 *Nature* **387** 686
[5] He J Y, Zhang Q Z, Wu X L and Chu P K 2013 *Chin. Phys. B* **22** 106804
[6] Pu H B, He X, Quan R D, Cao L and Chen Z M 2013 *Chin. Phys. B* **22** 037301
[7] Liu Z, Wang S, Otogawa N, Suzuki Y, Osamura M, Fukuzawa Y, Ootsuka T, Nakayama Y, Tanoue H and Makita Y 2006 *Sol. Energy Mater. Sol. Cells* **90** 276
[8] Shaban M, Nomoto K, Nakashima K, Izumi S and Yoshitake T 2008 *Appl. Phys. Lett.* **94** 222113
[9] Yuan J R, Shen H L, Lu L F, Huang H B and He X C 2010 *Physica B* **405** 4565
[10] Yuan J R, Shen H L and Lu L F 2011 *Physica B* **406** 1733
[11] Hou G, Yu C, Liu F, Sun J, Geng X and Zhao Y 2012 *Phys. Status Solidi C* **7** 1081
[12] Gao Y, Liu H, Lin Y and Shao G 2012 *Thin Solid Films* **519** 8490
[13] Yao W J, Zeng, X B, Peng, W B, Liu S Y, Xie X B, Wang C and Liao X B 2011 *Chin. Phys. B* **20** 078402
[14] Luque A and Hegedus S 2003 *Handbook of PV Science and Engineering* (Chichester: Wiley)
[15] Takimoto K, Fukuta A, Yamamoto Y, Yoshida N, Itoh T and Nonomura S 2002 *J. Non-Cryst. Solids* **299** 314
[16] Herz K, Powalla M and Eicke A 1994 *Phys. Status Solidi A* **145** 415
[17] Zhu H, Kalkan A K, Hou J and Fonash S J 1999 *AIP Conf. Proc.* **462** 309
[18] Rubinelli F A, Arch J K and Fonash S J 1992 *J. Appl. Phys.* **72** 1621
[19] Dutta U and Chatterjee P 2004 *J. Appl. Phys.* **96** 2261
[20] http://www.ampsmodeling.org/materialData_silicon.html [2013]
[21] Schropp R E I and Zeman M 1998 *Amorphous and Microcrystalline Silicon Solar Cells: Modeling, Materials and Device Technology* (New York: Springer)

[22] Searle T 1998 *Properties of Amorphous Silicon and Its Alloys* (London: Institution of Electrical Engineers)

[23] Vanecek M 1998 *J. Non-Cryst. Solids* **227/230** 967

[24] Cody G D, Tiedje T, Abeles B, Brooks B and Goldstein Y 1981 *Phys. Rev. Lett.* **47** 1480

[25] Kunii T, Yoshida N, Hori Y and Nonomura S 2006 *Jpn. J. Appl. Phys.* **45** 393

[26] Yang Z, Homewood K P, Finney M S, Harry M A and Reeson K J 1995 *J. Appl. Phys.* **78** 1958

[27] Yunaz I A, Sriprapha K, Hiza S, Yamada A and Konagai M 2007 *Jpn. J. Appl. Phys.* **46** 1398

[28] Huang Z H, Zhang J J, Ni J, Cao Y, Hu Z Y, Li C, Geng X H and Zhao Y 2013 *Chin. Phys. B* **22** 098803

[29] Zhang X D, Zheng X X, Xu S Z, Lin Q, Wei C C, Sun J, Geng X H and Zhao Y 2011 *Chin. Phys. B* **20** 108801

[30] Green M A, Emery K, Hishikawa Y, Warta W and Dunlop E D 2013 *Prog. Photovolt.: Res. Appl.* **21** 827

[31] Isomura M M, Wakisaka K, Murata K, Murata K and Tanaka M 2005 *Sol. Energy Mater. Sol. Cells* **85** 167

[32] Pankove J I 1971 *Optical Processes in Semiconductor* (New York: Dover)

[33] Marti A and Araujo G L 1996 *Sol. Energy Mater. Sol. Cells* **43** 203